Detection of Ozone on Ganymede

Keith S. Noll,* Robert E. Johnson, Arthur L. Lane,
Deborah L. Domingue, Harold A. Weaver

An absorption band at 260 nanometers on the trailing hemisphere of Ganymede, identified as the Hartley band of ozone (O_3), was measured with the Hubble Space Telescope. The column abundance of ozone, 4.5×10^{16} per square centimeter, can be produced by ion impacts or by photochemical equilibrium with previously detected molecular oxygen (O_2). An estimated number density ratio of $[O_3]/[O_2] \approx 10^{-4}$ to 10^{-3} requires an atmospheric density orders of magnitude higher than upper limits from spacecraft occultation experiments. Apparently, this O_2-O_3 "atmosphere" is trapped in Ganymede's surface ice, an inference consistent with the shift and broadening of the band compared with the gas-phase O_3 band.

Jupiter's three large icy satellites—Europa, Ganymede, and Callisto—orbit within the jovian magnetosphere. As a consequence, they are continually bombarded by charged particles trapped in Jupiter's magnetic field. All three satellites are tidally locked to Jupiter so that the same hemisphere of each moon is always pointed in the direction of orbital motion (the leading hemisphere) and the other in the opposite direction (the trailing hemisphere). The orbital velocities of the satellites are smaller than the corotation velocity, so the trailing hemispheres receive the largest flux of ions.

Many observed leading and trailing hemisphere dichotomies have been attributed to the preferential irradiation of the trailing hemispheres. Two bands of O_2 have been identified in visible-wavelength spectra with a marked increase on Ganymede's trailing hemisphere (*1*, *2*). Observations in the ultraviolet (UV) by the International Ultraviolet Explorer (IUE) identified smooth variations in UV albedo as a function of longitude for all three satellites (*3*). In addition, a spectral absorption feature centered at 280 nm on Europa's trailing hemisphere has been identified as SO_2 ice mixed with the dominantly H_2O-ice surface (*4–6*). The ratio of the IUE spectrum of Ganymede's trailing to that of its leading hemisphere showed evidence for a spectral absorber on Ganymede's trailing hemisphere as well (*3*), although the ratio continued to decrease below 280 nm to the limit of adequate signal near 260 nm. Nelson *et al.* (*3*) proposed that this absorption might be caused by a combination of SO_2 and O_3 produced by implantation of sulfur and oxygen ions in the surface of Ganymede. However, the inadequacy of IUE spectra below 260 nm made firm identification impossible. We have used the Hubble Space Telescope's Faint Object Spectrograph (FOS) to collect at high signal-to-noise ratios data to wavelengths as short as 210 nm, allowing us to detect O_3 and possibly other molecules in Ganymede's UV spectrum.

We observed Ganymede in two separate orbits with the FOS. The leading hemisphere was observed on 25 June 1995 at 18:39 and 18:47 UT, the trailing hemisphere on 6 July 1995 at 13:36 and 13:44 UT (*7*). We calculated the albedo spectra (Fig. 1) at the observed phase angle by dividing out the solar spectrum measured by the SOLSTICE experiment (*8*). The observations were made at phase angles of 4.8° and 6.7° for hemispheres centered at 71° (leading) and 255° (trailing), respectively. The spectra include features that result from variable solar lines, notably the Mg II doublet at 280 nm and Mg I at 285 nm. The albedos of both the leading and trailing hemispheres decrease at short wavelengths. The trailing hemisphere, however, reflects less than half the amount of light as does the leading hemisphere, and the overall shape of the spectra differ.

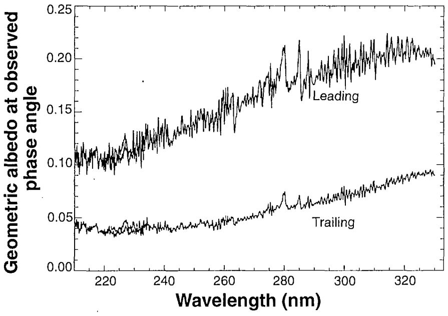

Fig. 1. Albedo spectra of Ganymede's leading and trailing hemispheres. The high-frequency structure results from incomplete removal of solar Fraunhofer lines because of small wavelength mismatches and variability in the solar lines. The uncertainty of the Ganymede spectrum is much smaller than this systematic noise. The G190H and G270H grating spectra overlap in a narrow interval near 225 nm. The G270H spectra are higher than the G190H spectra by 6 to 10%. We take this as an indicator of absolute flux uncertainty. The broad absorption present in the trailing hemisphere spectrum can be seen by comparing the relative slopes of the two curves.

To remove spectral features shared in common by the leading and trailing hemispheres, we produced a ratio spectrum: trailing/leading (Fig. 2). Because additional absorbers are present on the trailing hemisphere, the ratio spectrum can be directly compared to laboratory spectra of candidate absorbers. The ratio spectrum can be characterized as a single, very broad absorption feature centered at 258 ± 2 nm with a full width at half maximum (FWHM) of at least 90 nm. The FWHM is a lower limit because the band appears to extend beyond the wavelength interval covered by our data.

The location of the absorption maximum coincides with the strong Hartley band of O_3 shifted to a slightly longer wavelength and broadened. In the laboratory, the Hartley band center shifts when O_3 is mixed with other materials; for example, a 6-nm shift to 260 nm occurs when O_3 is dissolved in H_2O (*9*). Vaida *et al.* (*10*) found that the FWHM of the Hartley band increases in H_2O solution (46 nm) and O_3 ice at 77 K (100 nm) compared with the 40-nm FWHM of O_3 gas. Thus, the shift and broadening of the O_3 band may be caused by O_3 trapped in Ganymede's surface ice.

We estimated the column abundance of O_3 by comparing model spectra to the ob-

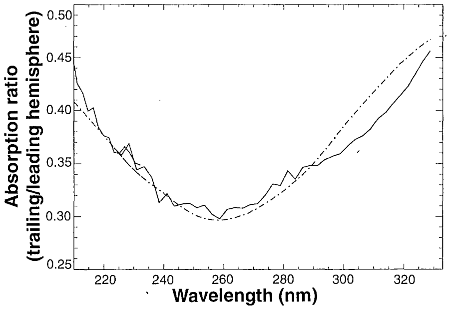

Fig. 2. Ratio of the spectrum of Ganymede's trailing hemisphere to that of its leading hemisphere (solid line). The FOS data have been rebinned to a spectral resolution of 2.5 nm. Also shown is a model spectrum (dash-dotted line) with an O_3 column abundance of $N = 4.5 \times 10^{16}$ cm^{-2}, calculated as described in the text. The uncertainty of the column abundance from the fitting process is about $\pm 1.5 \times 10^{16}$ cm^{-2}, but we estimate the total uncertainty to be an order of magnitude, dominated by the lack of cross sections for O_3 in ice at the appropriate conditions.

K. S. Noll, Space Telescope Science Institute, 3700 San Martin Drive, Baltimore, MD 21218, USA.
R. E. Johnson, University of Virginia, Nuclear Engineering and Engineering Physics, Charlottesville, VA 22901, USA.
A. L. Lane, Jet Propulsion Laboratory, 4800 Oak Grove Drive, Pasadena, CA 91109, USA.
D. L. Domingue, Lunar and Planetary Institute, 3600 Bay Area Boulevard, Houston, TX 77058, USA.
H. A. Weaver, Johns Hopkins University, Department of Physics and Astronomy, Baltimore, MD 21218, USA.

*To whom correspondence should be addressed.

served ratio spectrum. We attempted to reproduce the effects of low temperature and close proximity to an H_2O matrix by doubling the FWHM of a measured O_3-gas cross section to 80 nm and shifting it by +6 nm. We then produced a comparison spectrum $y = y_0e^{-N\sigma}$, where y_0 is a constant chosen to allow for additional, wavelength-independent darkening of the trailing hemisphere, σ is the O_3 cross section, and N is the total column abundance of O_3 encountered by the photons we detect. Solving for N, we find a good fit for $N \approx 4.5 \times 10^{16}$ cm^{-2} and $y_0 = 0.5$. Because we lacked measured cross sections for O_3 in ice, this value should be considered as an estimate good to within an order of magnitude.

We also produced models that included absorption from SO_2 ice (*5*) at 280 nm in addition to the absorption from O_3. We determined an upper limit of $N(SO_2) < 3 \times 10^{16}$ cm^{-2}. This limit is less than 20% of the amount of SO_2 observed on Europa's trailing hemisphere (*6*). For this abundance, the model produces a poor fit to the observed spectrum, with the band shifted to ≈268 nm and too much absorption between 265 and 285 nm. At smaller abundances the distortion of the combined bands is less apparent, although SO_2 does cause a slight shift in the center of the feature to longer wavelengths. Some or all of the shift we observe in the O_3 band center may be caused by small quantities of SO_2.

An additional feature in the ratio spectrum (Fig. 2) not present in the model O_3 spectrum is centered at about 310 nm with a FWHM ≈ 30 nm and a peak absorption depth of 8%. The position of the band suggests the strong A-X band of OH, which is centered at 309 nm in the gas phase (*11*). Because OH is a predicted product of photolysis and irradiation of H_2O ice (*12*), it is a reasonable candidate for this band. However, the OH band in a solid H_2O matrix is shifted (*12*) to 280 nm.

We did not find any evidence in the ratio spectrum for HO_2 at 230 to 235 nm or for H_2O_2, which peaks at a wavelength just short of our range (*12*). Because H_2O_2 is produced in UV-irradiated laboratory samples of O_3 in H_2O ice (*13*), it might be expected to occur on Ganymede. However, the source of the red slope in the UV spectra of icy satellites is not fully understood, and these two gases could be contributors (*14*). Laboratory studies of ice irradiated by He^+ ions show a reddening at wavelengths $\lambda <$ 500 nm (*5, 15*). Spectra of these satellites at wavelengths shorter than 210 nm could identify the presence of these molecules.

Ozone is surprisingly abundant on Ganymede. The O_2 absorptions observed on Ganymede have been estimated as equivalent to those of a 20- to 200-μm layer (*2*) of solid O_2. Assuming that visible and UV photons traverse the same path length in the ice, we find a number density ratio of $[O_3]/[O_2] \approx 4 \times 10^{-4}$, 10 times the peak ratio in Earth's stratosphere (*16*). Because the observed Hartley band results in dissociation of O_3, the column abundance of O_3 must represent a balance between active production and destruction of O_3 in Ganymede's surface. Using our estimate of the equilibrium ratio of O_3 to O_2 and the oxygen-only Chapman reactions (*17*), we can eliminate the possibility that O_3 is present in an atmosphere above Ganymede's surface. For $[O_3]/[O_2] >> 1.3 \times 10^{-7}$, the ratio of O_3 to O_2 is given by $[O_3]/[O_2] = (k_{12}J_2[M]/k_{13}J_3)^{1/2}$, where [M], the number density of nearby molecules able to participate in the three-body reaction, is unknown. Ratios $[O_3]/[O_2]$ of order 10^{-4} to 10^{-3} require $[M] \approx 10^{14}$ to 10^{16} cm^{-3}. An atmosphere of this density was ruled out by the Voyager occultation experiment (*18*), which established an upper limit of 6×10^8 cm^{-3}. We interpret this unlikely value as further evidence supporting the hypothesis that the O_3 we observed is trapped in voids in Ganymede's surface ice. A more complete analysis of possible reaction paths is required to account for reactions relevant at high $[O_3]$ not included in the Chapman model, particularly $O(^1D)$ quenching of O_3.

Ozone is produced by ion irradiation and photolysis of O_2. Although direct production of O_3 by ion irradiation of ice has not been reported, we estimate a time scale t for the production of the observed excess O_3 column abundance from $N = \varepsilon\Delta\Phi t$. The number of O_3 molecules produced per incident ion is represented by ε and $\Delta\Phi$ is the additional ion flux on the trailing hemisphere. Calvin *et al.* (*2*) fitted the longitudinal variation of O_2 with a four-to-one mix of corotating and hot plasma with average ion energies of 1.5 and 30 keV, respectively. For a corotation ion flux of 2×10^8 cm^{-2} s^{-1}, the excess energy flux on the trailing hemisphere is ≈10^9 keV cm^{-2} s^{-1} with an average ion energy of 7 keV. Assuming one O_3 formed per 1 keV deposited [a G value (*19*) of 0.1], then $\varepsilon = 7$ and $t = 10^7$ s, which is short compared with the age of Ganymede's surface. Equilibration time scales for O_3 produced by photolysis of O_2 are comparably short.

The maintenance of an O_2-O_3 equilibrium on Ganymede can be described as an atmospheric process, although the atmosphere is a most unusual one. Several lines of evidence indicate that O_2 (*1, 2*) and O_3 exist in small voids in Ganymede's surface ice, where high effective densities can be achieved. Laboratory experiments suggest that O atoms diffuse through an ice lattice (*12*) and O_2 forms at interfaces. Thus, the gas we detect is likely to be located in cracks and bubbles in the ice rather than in individual lattice sites because the observations require the presence of more than one O_2 molecule. Some of the O_2 and O_3 must escape from the ice; a tenuous oxygen atmosphere, similar to the one recently identified on Europa (*20*), is likely (*19*).

The concentration of O_3 and O_2 on Ganymede's trailing hemisphere and SO_2 on Europa's indicates that these molecules are products, either direct or indirect, of ion bombardment. Compositional and energy differences of the impacting ions may be responsible for the difference in the composition of the irradiation products between Ganymede and Europa. Io is the main source of heavy ions, mainly S and O, in the jovian magnetosphere, with Europa being a smaller source of O ions. At Europa, the ratio of S/O ions in the satellite orbit plane is 0.6 to 0.8 (*21, 22*), and the O/He ratio is 1.5 (*22*). At Ganymede, the ion density is lower, the ratio of S/O decreases by a factor of 2, and the O/He ratio decreases by a factor of 5 (*22*). Thus, the fraction of S in the heavy-ion flux is reduced by an order of magnitude at Ganymede relative to that at Europa. If implanted S ions are ultimately responsible for the formation of SO_2 on Europa, this decrease may explain the absence of SO_2 on Ganymede.

On the other hand, the presence of O_3 on Ganymede but SO_2 on Europa may reflect differences in the composition of the surface ices of these two satellites rather than in the composition of the plasma. In particular, Europa may contain a higher abundance of sulfur in its surface ices than does Ganymede. Europa has been thermally processed to a greater extent than has Ganymede, and Europa's higher density indicates that a greater fraction of its initial inventory of water has been lost. Io represents an even more extreme example of thermal processing, one where the next most volatile component after water ice, sulfur, is a major surface component. The albedo spectra of Ganymede and Europa drop at wavelengths shorter than $\lambda \approx 600$ nm, but they differ in detail. The spectra of both the leading and trailing hemispheres of Europa can be matched with a spectrum of mixed sulfur compounds (*1*), so the sulfur may be endogenic.

The Hartley band of O_3 is intrinsically much stronger than the two weak bands of O_2 found in Ganymede's spectrum (*1, 2*) and therefore is a more sensitive indicator of the presence of O_2-O_3 systems in other icy satellites. Saturn's satellites Rhea, Dione, and Tethys are known to have surfaces dominated by water ice (*23*) and trailing hemispheres that show symmetric dark regions centered on the antapex of orbital motion (*24*), suggestive of alteration by magnetospheric ion irradiation. Magnetospheric ion densities are comparable to densities found near Europa and Ganymede (*19*). Thus, these satellites are good candidates for searches for O_3 absorption that will test the range of environmental conditions under which O_2-O_3 systems can be formed.

Bodies with icy surfaces are, by far, the most numerous objects in the solar system. Other planetary systems are also, probably, dominated by icy objects. Ganymede is a world with a diameter 40% the diameter of Earth where an abundance of O_3 has been produced, through an inorganic process, that is a not insignificant fraction of that in Earth's atmosphere. Searches for Earth-like planets harboring life similar to life on our planet that rely on the detection of O_3 (*25*) will have to take this process into account.

REFERENCES AND NOTES

1. J. R. Spencer, W. M. Calvin, M. J. Person, *J. Geophys. Res.* **100**, 19049 (1995).
2. W. H. Calvin, R. E. Johnson, J. R. Spencer, *Geophys. Res. Lett.* **23**, 673 (1996).
3. R. M. Nelson *et al.*, *Icarus* **72**, 358 (1987).
4. A. L. Lane, R. M. Nelson, D. L. Matson, *Nature* **292**, 38 (1981).
5. N. J. Sack, R. E. Johnson, J. W. Boring, R. A. Baragiola, *Icarus* **100**, 534 (1992). We use a density of 1.4 g cm^{-3} for SO_2 ice. The band at 280 nm observed for incident He^+ is probably trapped OH and not O_2, as is suggested by Sack *et al.*
6. K. S. Noll, H. A. Weaver, A. M. Gonnella, *J. Geophys. Res.* **100**, 19057 (1995).
7. On both dates we observed through the G270H grating (λ = 220 to 330 nm) and the G190H grating (λ = 155 to 230 nm) for a total of 130 and 1080 s, respectively. All observations were made through the 0.86–arc sec–diameter circular aperture while the telescope tracked Ganymede. We used the blue digicon detector assay (FOS/BL); scattering within the grating dominated the detected signal at wavelengths below 210 nm. Ganymede was located with the Goddard High Resolution Spectrograph, after which we slewed to the FOS to make the observations. The expected precision of the final pointing is 0.1 arc sec. When we located Ganymede's trailing hemisphere, the final fine *x*-null balance was not completed, possibly because of bright, off-center albedo features. However, the ratio of trailing to leading hemisphere flux agrees with that found by IUE (*3*), indicating that the 0.86–arc sec aperture was filled by the 1.62–arc sec–diameter disk of Ganymede. We corrected the pipeline calibrated fluxes provided by the Space Telescope Science Institute to account for the fact that the angular size of Ganymede was larger than the aperture.
8. G. J. Rottman, private communication.
9. H. Taube, *Trans. Faraday Soc.* **53**, 656 (1956).
10. V. Vaida, D. J. Donaldson, S. J. Strickler, S. L. Stephens, J. W. Birks, *J. Phys. Chem.* **93**, 506 (1989).
11. D. G. Schleicher and M. F. A'Hearn, *Astrophys. J.* **331**, 1058 (1988).
12. A. J. Matich, M. G. Bakker, D. Lennon, T. I. Quickenden, C. G. Freeman, *J. Phys. Chem.* **97**, 10539 (1993).
13. A. J. Sedlacek and C. A. Wight, *ibid.* **93**, 509 (1989).
14. A. L. Lane, D. L. Domingue, S. K. Price, M. Lankton, *Bull. Am. Astron. Soc.* **26**, 1159 (1994).
15. N. J. Sack, J. W. Boring, R. E. Johnson, R. A. Baragiola, M. Shi, *J. Geophys. Res.* **96**, 17535 (1991).
16. The bracket notation is used to indicate number density. The ratio would be even larger if the shorter UV path length implied by the low UV albedo were taken into account. However, the estimate of the $[O_3]/[O_2]$ ratio is uncertain by at least an order of magnitude, so additional refinements are unwarranted at this point.
17. A description of the Chapman reaction sequence can be found in J. W. Chamberlain and D. M. Hunten, *Theory of Planetary Atmospheres: An Introduction to Their Physics and Chemistry* (Academic Press, Orlando, FL, ed. 2, 1987). For the reaction $O + O_2 + M \rightarrow O_3 + M$, we use a rate $k_{12} = 6.0 \times 10^{-34}(T/300)^{-2.3}$ $cm^6\ s^{-1}$, or 4×10^{-33} $cm^6\ s^{-1}$ for an assumed temperature T of 130 K. The reaction rate for $O + O_3 \rightarrow 2O_2$ is $k_{13} = 8.0 \times 10^{-12}\ e^{-2060/T}$ $cm^3\ s^{-1}$, which is 1×10^{-18} $cm^3\ s^{-1}$ at 130 K. Photodissociation rates are affected by the extinction of UV flux in the ice layers. We used photodissociation rates for Earth's atmosphere at 60 km, where the overlying mass column abundance is roughly equivalent to a 1-cm-thick layer of ice, scaled by a factor of 0.074 to remove the diurnal variation and account for the reduced solar flux at Jupiter. For $O_2 + h\nu \rightarrow O + O$ (where $h\nu$ is the energy of a photon), we use the rate $J_2 = 4 \times 10^{-11}\ s^{-1}$, and for $O_3 + h\nu \rightarrow O + O_2$, we use $J_3 = 3 \times 10^{-4}\ s^{-1}$. The ratio J_2/J_3 is less sensitive to assumptions about UV extinction than are the individual rates. The Chapman reaction sequence is valid for gas-phase chemistry. Here we have used it to indicate high total densities that imply the O_2-O_3 system is located in high-density pockets within the surface ice. Thus, a full analysis of the chemistry will have to include reactions that take place on solid surfaces.
18. A. L. Broadfoot *et al.*, *Science* **204**, 979 (1979). The value of [M] derived by our method, although highly uncertain, cannot be made to agree with the occultation upper limits even for extreme assumptions about the possible uncertainty of $[O_3]/[O_2]$.
19. R. E. Johnson, *Energetic Charged Particle Interactions with Atmospheres and Surfaces* (Springer, Berlin, 1990).
20. D. T. Hall, D. F. Strobel, P. D. Feldman, M. A. McGrath, H. A. Weaver, *Nature* **373**, 677 (1995).
21. F. Bagenal, D. E. Shemansky, R. L. McNutt Jr., R. Schreier, A. Eviatar, *Geophys. Res. Lett.* **19**, 79 (1992).
22. D. C. Hamilton, G. Gloeckler, S. M. Krimigis, L. J. Lanzerotti, *J. Geophys. Res.* **86**, 8301 (1981).
23. T. L. Roush, D. P. Cruikshank, T. C. Owen, in *Volatiles in the Earth and Solar System*, K. A. Farley, Ed. (American Institute of Physics, Washington, DC, 1995), pp. 143–153; R. N. Clark, R. H. Brown, P. D. Owensby, A. Steele, *Icarus* **58**, 265 (1984).
24. B. J. Buratti, J. A. Mosher, T. V. Johnson, *Icarus* **87**, 339 (1990).
25. B. F. Burke, *Nature* **322**, 340 (1986); A. Léger, M. Pirre, F. J. Marceau, *Astrophys. Space Sci.* **212**, 327 (1994); C. Sagan, W. R. Thompson, R. Carlson, D. Gurnett, C. Hord, *Nature* **365**, 715 (1993). Sagan *et al.* point out that the detection of disequilibrium O_3 is not, in itself, evidence of life.
26. We thank W. Calvin and J. Joiner for several enlightening discussions. These observations were supported by grant GO-5837 from the Space Telescope Science Institute, which is operated by the Association of Universities for Research in Astronomy under NASA contract NAS5-26555.

4 March 1996; accepted 29 May 1996

Self-Assembled Smectic Phases in Rod-Coil Block Copolymers

J. T. Chen, E. L. Thomas,* C. K. Ober,* G.-p. Mao

Rod-coil block copolymers are self-assembling polymers that combine the physics of orientational ordering of rodlike polymers and the microphase separation of coil-coil block copolymers. Several new solid-state morphologies were observed in a series of anionically synthesized model poly(hexyl isocyanate-b-styrene) rod-coil diblock copolymers examined by transmission electron microscopy and selected-area electron diffraction. The rod-coils formed smectic C-like and O-like morphologies with domain sizes ranging from tens of nanometers to almost 1 micrometer. Both structural and orientational changes were found for increasing rod volume fractions. In addition, some morphologies exhibited spontaneous long-range orientational order over many tens of micrometers.

In recent years, much work has focused on the morphology and phase behavior of block copolymers. The simplest copolymers are AB diblock copolymers, which are made up of two chemically distinct blocks covalently bonded together to form a single chain. Because of the mutual repulsion of dissimilar monomers and the constraint imposed by the connectivity of the A block with the B block, coil-coil diblocks (both blocks flexible) exhibit a wide range of microphase-separated morphologies (*1*). The parameters that determine the morphology of a given block copolymer (*2*) are the Flory-Huggins interaction parameter, χ_{AB}; the total degree of polymerization, $N = N_A + N_B$; and the volume fraction (composition) of the A component, f_A. The parameter χ_{AB} is a measure of the incompatibility between the A and B polymers and is inversely proportional to temperature.

Rodlike homopolymers have also been extensively studied. In contrast to flexible homopolymers, which obey Gaussian chain statistics and have persistence lengths of ~1 nm, rodlike polymers have nearly linear chain conformations and large persistence lengths ranging from 10 to 100 nm. The inherent chain stiffness of rodlike polymers

---

J. T. Chen and E. L. Thomas, Department of Materials Science and Engineering, Massachusetts Institute of Technology, Cambridge, MA 02139, USA.
C. K. Ober and G.-p. Mao, Department of Materials Science and Engineering, Cornell University, Ithaca, NY 14853, USA.

*To whom correspondence should be addressed.